The Astrophysical Journal, 786:112 (9pp), 2014 May 10 doi:10.1088/0004-637X/786/2/112

BIG BANG NUCLEOSYNTHESIS REVISITED VIA TROJAN HORSE METHOD MEASUREMENTS

R. G. Pizzone[1], R. Spartá[1,2], C. A. Bertulani[3], C. Spitaleri[1,2], M. La Cognata[1], J. Lalmansingh[3], L. Lamia[2], A. Mukhamedzhanov[4], and A. Tumino[1,5]
[1] INFN—Laboratori Nazionali del Sud, Via Santa Sofia 62, I-95123 Catania, Italy; rgpizzone@lns.infn.it
[2] Dipartimento di Fisica e Astronomia, Università degli Studi di Catania, Via Santa Sofia 64, I-95123 Catania, Italy
[3] Department of Physics and Astronomy, Texas A&M University, Commerce, TX 75025, USA
[4] Cyclotron Institute, Texas A&M University, College Station, TX 77843, USA
[5] Università degli Studi di Enna "Kore," Via delle Olimpiadi, I-94100 Enna, Italy
Received 2014 February 7; accepted 2014 March 18; published 2014 April 24

ABSTRACT

Nuclear reaction rates are among the most important input for understanding primordial nucleosynthesis and, therefore, for a quantitative description of the early universe. An up-to-date compilation of direct cross-sections of ^{2}H$(d, p)^3$H, ^{2}H$(d, n)^3$He, ^{7}Li$(p, \alpha)^4$He, and ^{3}He$(d, p)^4$He reactions is given. These are among the most uncertain cross-sections used and input for big bang nucleosynthesis calculations. Their measurements through the Trojan Horse method are also reviewed and compared with direct data. The reaction rates and the corresponding recommended errors in this work were used as input for primordial nucleosynthesis calculations to evaluate their impact on the ^{2}H, ^{3,4}He, and ^{7}Li primordial abundances, which are then compared with observations.

Key words: early universe – nuclear reactions, nucleosynthesis, abundances – primordial nucleosynthesis

Online-only material: color figures

1. INTRODUCTION

Over recent decades, big bang nucleosynthesis (BBN) has emerged as one of the pillars of the big bang model, together with the Hubble expansion and the cosmic microwave background (CMB) radiation Steigman (2007). BBN probes the universe to the earliest times, from a fraction of a second to a few minutes. It involves events that occurred at temperatures below 1 MeV, and naturally plays a key role in forging the connection between cosmology and nuclear physics (Fields & Sarkar 2006). Focusing only on the products of the BBN, according to the standard big bang nucleosynthesis (SBBN) model, only the formation of light nuclei (^{2}H,^{3,4}He,^{7}Li) is predicted in observable quantities, starting from protons and neutrons. Today, with the only exceptions of ^{3}He and lithium, the abundances of these isotopes in the appropriate astrophysical environments are rather consistent with SBBN predictions (Israelian 2012). A comparison between the primordial abundances from *Wilkinson Microwave Anisotropy Probe* (*WMAP*) observations and the calculated ones constrains the baryon-to-photon ratio, η, which is the only free parameter in the presently accepted model of the SBBN. A recent observation yields $\eta = 6.16 \pm 0.15 \times 10^{-10}$ (Komatsu et al. 2011), which is the value that we adopt in our calculations.

BBN requires several nuclear physics inputs and, among them, an important role is played by nuclear reaction rates. Due to the relatively small amount of key nuclear species involved in the BBN nuclear reaction network, only 12 reactions play a major role (Kolb & Turner 1990). They are listed in Table 1.

The reaction rates are calculated from the available low-energy cross-sections for the reactions. This is also fundamental information for a number of other unsolved astrophysical problems, e.g., the so-called "lithium depletion" either in the Sun or in other galactic stars (Weymann & Moore 1963; Ezer & Cameron 1963). Cross-sections should be measured in the astrophysically relevant Gamow window (Iliadis 2007; Bertulani 2013), of the order of a few hundreds keV. In the last decades, these reactions have been widely studied and, in particular, great efforts have been devoted to their study by means of direct measurements at relevant astrophysical energies, sometimes in underground laboratories (Bonetti et al. 1999; Casella et al. 2002) or improved detection systems.

For these extreme low-energy cross-section measurements, and in several physical cases, new phenomena, such as the electron screening effect, can no longer be neglected. These can significantly alter the low-energy cross-section in direct experiments (Assenbaum et al. 1987) due to the partial screening of nuclear charges by atomic electron clouds. For applications to astrophysical plasmas one needs the "bare nucleus" cross-section, σ_b, especially because the screening in stellar conditions is much different from that in the laboratory.

Moreover, for many of the relevant reactions, no direct experiments exist at astrophysical energies (mostly because of difficulties connected with the presence of the Coulomb barrier in charged particle-induced reactions) and the cross-section within the Gamow window has to be extrapolated from higher energy measurements. Alternative, and challenging, ways to obtain σ_b for charged particles at sub-Coulomb energies have been provided by indirect methods such as the Coulomb dissociation method (Baur et al. 1986; Bertulani & Gade 2010) and the asymptotic normalization coefficient (Mukhamezhanov et al. 2008). Among them, the Trojan Horse method (THM; Spitaleri et al. 1999, 2003, 2001) is particularly suited to investigate binary reactions induced at astrophysical energies by neutrons or charged particles by using appropriate three-body reactions. It allows one to avoid both Coulomb barrier suppression and electron screening effects, thus preventing the use of unreliable extrapolations.

An experimental program has been carried out during the last decade to apply the THM to study reactions of relevance for the SBBN (reactions marked in Table 1 with a $^{(*)}$). In the next sections, we will first discuss the available direct data for these four reactions in order to calculate their rate. In a subsequent section we will show the calculations of the reaction rates based

Table 1
Nuclear Reactions of Greatest Relevance for Big Bang Nucleosynthesis, Labeled from 1 to 12

$n \leftrightarrow p$ (1)	$p(n,\gamma)d$(2)	$d(p,\gamma)^3$He (3)	$d(d,p)t^{(*)}$(4)
$d(d,n)^3\mathrm{He}^{(*)}$ (5)	$^3\mathrm{He}(n,p)t$ (6)	$t(d,n)^4$He (7)	$^3\mathrm{He}(d,p)^4\mathrm{He}^{(*)}$ (8)
$^3\mathrm{He}(\alpha,\gamma)^7$Be (9)	$t(\alpha,\gamma)^7$Li (10)	^{7}Be(n, p)^{7}Li (11)	$^7\mathrm{Li}(p,\alpha)^4\mathrm{He}^{(*)}$ (12)

Note. Reactions measured with the Trojan Horse method are marked with a (∗) symbol.

also on the THM measurements of the cross-sections, σ_b. The THM has been applied to several reactions in the past decade (Tumino et al. 2008; Lamia et al. 2013, 2007, 2012c, 2012a; La Cognata et al. 2005, 2011; Sergi et al. 2010; Romano et al. 2006; Wen et al. 2008; Pizzone et al. 2005b, 2009), at the energies relevant for astrophysics, which usually are far below the Coulomb barrier, of the order of MeVs. Many tests have been made to fully explore the potentiality of the method and extend its applications as much as possible: the target/projectile break-up invariance (Musumarra et al. 2001), the spectator invariance (Tumino et al. 2006; Pizzone et al. 2011, 2013), and the possible use of virtual neutron beams (Tumino et al. 2005; Gulino et al. 2010). Such studies are necessary, as the THM has become one of the major tools for the investigation of reactions of astrophysical interest (for recent reviews see Spitaleri et al. 2011). Thus, the method can be regarded as a powerful indirect technique to get information about the bare nucleus cross-section for reactions of astrophysical interest, which leads to the determination of new reaction rates.

2. *S*-FACTORS AND REACTION RATES

The energy dependence of the bare nucleus cross-sections is usually expressed in terms of the equation

$$\sigma_b(E) = \frac{S(E)}{E} \exp\left(-2\pi\eta E\right), \tag{1}$$

where $S(E)$ is the astrophysical factor (or simply S-factor), $\eta = Z_i Z_j e^2/\hbar v$ is the Sommerfeld parameter, with Z_i as the ith nuclide charge, v as the relative velocity of the ij-pair, and $E = \mu v^2/2$ as the relative energy of $i+j$. The S-factor has a relatively weak dependence on the energy E, except when it is close to a resonance, where it is strongly peaked. Using standard nuclear physics units, we write $2\pi\eta = b/\sqrt{E}$, where

$$b = 0.9898 Z_i Z_j \sqrt{A}\ \mathrm{MeV}^{1/2}, \tag{2}$$

and A is the reduced mass of $i+j$ in amu.

The thermonuclear reaction rate at temperature, T, is obtained from an average over the Maxwellian velocity distribution (Fowler et al. 1967):

$$R_{ij} = \frac{N_i N_j}{1+\delta_{ij}}\langle\sigma v\rangle = \frac{N_i N_j}{1+\delta_{ij}}\left(\frac{8}{\pi A}\right)^{\frac{1}{2}}\left(\frac{1}{k_B T}\right)^{\frac{3}{2}} \times \int_0^\infty dE\, S(E) \exp\left[-\left(\frac{E}{k_B T} + 2\pi\eta(E)\right)\right], \tag{3}$$

where σ is the fusion cross-section, v is the relative velocity of the ij-pair, and N_i is the number of nuclei of species, i. The factor $1+\delta_{ij}$ in the denominator of Equation (3) corrects for the double-counting when $i = j$.

We will express our reaction rates in the form $N_A\langle\sigma v\rangle$ (in units of cm^3 mol^{-1} s^{-1}), where N_A is the Avogadro number and $\langle\sigma v\rangle$ involves the integral in Equation (3) with the Maxwell distribution. For charged particles, a good accuracy (within 0.1%) is reached using the integration limits between $\max(0, E_0 - 5\Delta E)$ and $E_0 + 5\Delta E$, where in terms of T_9 (temperature in units of 10^9 K), the effective Gamow energy is given by

$$E_0 = 0.122\left(Z_i^2 Z_j^2 A\right)^{1/3} T_9^{2/3}\ \mathrm{MeV}, \tag{4}$$

and the Gamow energy window by

$$\Delta E = 0.2368\left(Z_i^2 Z_j^2 A\right)^{1/6} T_9^{5/6}\ \mathrm{MeV}. \tag{5}$$

2.1. *R*-matrix Fit

In contrast to polynomial fitting, the R-matrix method uses basic quantum mechanics as a guide for the data fitting and, therefore, is a preferable method. R-matrix fits are particularly useful in the presence of resonances. The energy dependence of the cross-sections arises from matching the solutions of the Schrödinger equation at a fixed distance from the origin (channel radius). Cross-sections and phase shifts are then reproduced with a small number of parameters (depending on the channel radius, a), allowing for an extrapolation of the cross-section down to astrophysical energies. The channel radius divides the space into two regions: the internal region (with radius, a), where nuclear forces are relevant, and the external region, where the interaction between the nuclei is governed by the Coulomb force. The R-matrix fits are usually weakly dependent on the channel radius. Matching at the channel radius leads to a number, N, of S-matrix poles characterized by energy, E_λ, and reduced width, $\tilde{\gamma}_\lambda$. The R-matrix at energy, E, is defined as

$$R_{ij}(E) = \sum_{\lambda=1}^{N} \frac{\tilde{\gamma}_{\lambda i}\tilde{\gamma}_{\lambda j}}{E_\lambda - E}, \tag{6}$$

where the indices i and j refer to the reaction channels. These also involve total momenta, J, and parities, π. The reduced widths are directly proportional to the square of the solutions of the Schrödinger equation for the internal region calculated at the channel radius, a.

From the R-matrix, one deduces the collision matrix with the help of which one can calculate the process of astrophysical interest, namely, radiative capture, transfer, elastic scattering, and rearrangement reactions. The R-matrix formula in Equation (6) can be used to fit both resonant and non-resonant reactions. For a non-resonant case, one uses a pole at large energies which simulates a background and yields an R-matrix almost independent of energy. A recent review of the R-matrix theory is found in Descouvemont & Baye (2010). In our fits, we use the multilevel, multichannel R-matrix public code, AZURE (Azuma et al. 2010). The code finds a best chi-square fit of the R-matrix parameters similar to Equation (8).

For the four reactions marked with a (*) symbol in Table 1, we have performed a function fit to the R-matrix output using direct and THM data (in the energy range where available, and using the direct data where not). The fit function was parameterized by a sum of polynomials and Breit–Wigner functions in the form

$$S_{\mathrm{fit}}(E) = \sum_{i=1}^{6} b_i E^{i-1} + \sum_{j=1}^{n_R} \frac{c_j}{(E-E_j)^2 + \Gamma_j^2/4} \quad (\mathrm{MeV}\cdot\mathrm{b}), \tag{7}$$

Table 2
Table of Fit Parameters (in Equation (7)) for the *S*-factors of the Reactions ^{2}H(d, p)^{3}H and ^{2}H(d, n)^{3}He Measured in TH Experiments, as Reported in the Text

Parameter	^{2}H(d, p)^{3}H	^{2}H(d, n)^{3}He
b_1	5.5325×10^{-2}	5.8613×10^{-2}
b_2	0.18293	0.18101
b_3	0.28256	0.44676
b_4	−0.62121	−0.8682
b_5	0.44865	0.61893
b_6	−0.11278	−0.15675

Note. The coefficients b_i are given in terms of MeV and barns.

where n_R is the number of resonances in the fit, E_j (in MeV) are the resonance energies and Γ_j (in MeV) are their widths. We applied the ordinary χ^2 statistics, defined by the minimization of

$$\chi^2 = \sum_i \frac{[S_{\rm exp}(E_i) - S_{\rm fit}(E_i; b_1, c_1, E_{R1}, \Gamma_1, \ldots)]^2}{\sigma_i^2}, \quad (8)$$

where $S_{\rm exp}(E_i)$ are the *S*-factors at energies, E_i, σ_i are the measured errors, and $S_{\rm fit}$ given by Equation (7). The fit function is then used in the calculation of the reaction rates using Equation (3).

3. BBN WITH TROJAN HORSE DATA

The reactions of interest for the SBBN cited in the introduction, i.e., ^{7}Li(p, α)^{4}He, ^{2}H(d, p)^{3}H, ^{2}H(d, n)^{3}He, and ^{3}He(d, p)^{4}He, were studied by means of the THM in the energy range of interest and their measurements were performed in an experimental campaign, which took place in the last decade (Pizzone et al. 2003, 2005a, 2005b, 2009; La Cognata et al. 2005, 2011; Sergi et al. 2010; Lamia et al. 2007, 2012c, 2012a; Romano et al. 2006; Wen et al. 2008). We will not go into the details of the THM because this is done elsewhere (Spitaleri et al. 2001), but we want to point out that the THM provides the bare $S(E)$ factor, i.e., free of screening effects, for the reaction under investigation after studying an appropriate three-body one in quasi-free (QF) kinematical conditions. The basic idea of the THM is to extract the cross-section in the low-energy region of a two-body reaction with significant astrophysical impact:

$$a + x \rightarrow c + C \quad (9)$$

from a suitable three-body QF reaction:

$$a + b \rightarrow s + c + C. \quad (10)$$

We therefore consider an interaction between the impinging nucleus and one of the clusters constituting the target (called participant x), while the residual nucleus, or spectator, does not participate in the reaction. In all the examined cases, the extracted astrophysical $S(E)$ factors were compared after the normalization procedure with those available from direct measurements and showed to be in fair agreement in the region where screening effects are negligible. The function fit parameters to the $S(E)$ factors, obtained with Equation (7) for the four reactions of relevance for BBN are listed in Tables 2 and 3 in units of MeV and barns. We will now review the available results for each reaction, taking into account the direct measurements available in the literature as well as the new THM results mentioned above.

Table 3
Table of Fit Parameters (in Equation (7)) for the *S*-factors of the Reactions ^{3}He(d, p)^{4}He and ^{7}Li(p, α)^{4}He Measured in TH Experiments

Parameter	^{3}He(d, p)^{4}He	^{7}Li(p, α)^{4}He
b_1	1.7096	-2.8141×10^{-2}
b_2	−20.121	2.6584×10^{-2}
b_3	38.975	-2.7907×10^{-2}
b_4	−20.406	-1.9457×10^{-3}
b_5	⋯	9.4651×10^{-4}
b_6	⋯	-5.0471×10^{-4}
c_1	0.49562	0.3198
E_{R1}	0.24027	2.5765
Γ_{R1}	0.35011	1.1579
c_2	⋯	9.7244×10^{-2}
E_{R2}	⋯	5.0384
Γ_{R2}	⋯	0.79323
c_3	⋯	0.40377
E_{R3}	⋯	6.0159
Γ_{R3}	⋯	1.8935
c_4	⋯	1.9247
E_{R4}	⋯	8.0614
Γ_{R4}	⋯	4.0738

Notes. The coefficients b_i and c_i are given in terms of MeV and barns. Energies and widths are in units of MeV.

3.1. $^2H(d, p)^3H$

The $d+d$ cross-section has been extensively measured in laboratory for each of the two *mirror channels*, ^{2}H(d, p)^{3}H and ^{2}H(d, n)^{3}He. Considering only results with a center-of-mass energy of interest for our purpose (i.e., around 1 MeV), the direct choice of data has been done accurately, selecting the newest and most reliable data sets, taking into account the possible presence of systematic errors. For ^{2}H(d, p)^{3}H, we chose the ones reported in Greife et al. (1995), Krauss et al. (1987), McNeill & Keyser (1951), Schulte et al. (1972), Jarmie & Brown (1990), Ganeev (1957), Arnold et al. (1954), Raiola et al. (2002), Booth et al. (1956), Davenport (1953), Von Engel (1961), Cook et al. (1953), Moffat (1952), and Tie-Shan (2007) and the most recent result from Leonard et al. (2006).

For the ^{2}H(d, p)^{3}H, the data set of Greife et al. (1995) reaches down to a center-of-mass energy value of 1.62 keV, but this experiences a clear enhancement for very low energies due to the electron screening effect. Thus, in order to be used for astrophysical application, they need to be corrected for this effect. It is also noticeable that the energy range between 600 keV and 1 MeV is not covered by any data set, making it difficult to provide a reliable fit in the whole energy range.

The TH experiment for this channel has been performed in two runs by measuring the three-body reaction ^{2}H(^{3}He, pt)H. The data analysis, performed according to the THM prescriptions, allowed for the measurement of the bare nucleus *S*-factor in the energy range from 2.6 keV up to 1.5 MeV, with a 5% error (a full review is given in Tumino et al. 2011, 2014).

In Figure 1, we show the data for the *S*-factor for the reaction ^{2}H(d, p)^{3}H obtained with the THM (blue filled circles) and by different direct measurements (red circles). The solid line is an *R*-matrix fit to both direct and indirect data, as described in Section 2.1. The parameters for an equivalent polynomial fit, using Equation (7), are listed in Table 2.

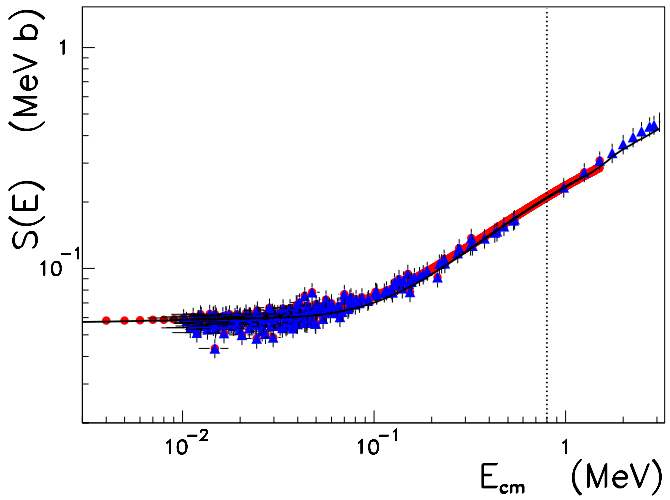

Figure 1. Experimental data for the *S*-factor obtained for the reaction ^{2}H(d, p)^{3}H with direct methods (blue solid triangles) and with the Trojan Horse method (red solid circles) data taken from Tumino et al. (2011, 2014). The solid line is an *R*-matrix fit following described in Section 2.1. The parameters for an equivalent polynomial fit are listed in Table 2. The vertical dotted line marks the upper value of the energy range of interest for primordial nucleosynthesis.

(A color version of this figure is available in the online journal.)

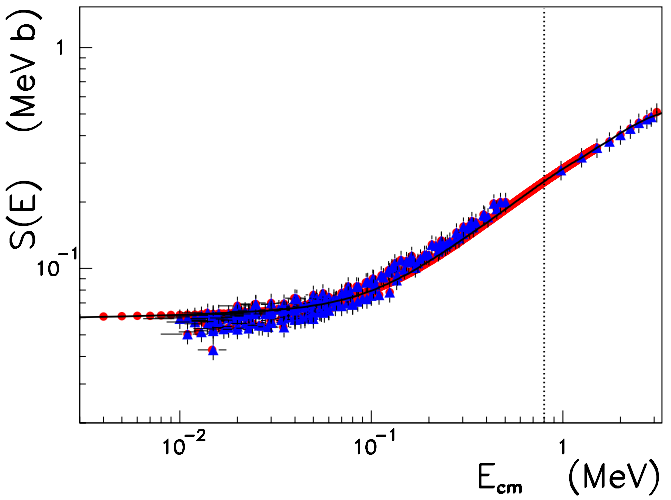

Figure 2. Experimental data for the *S*-factor of the reaction, ^{2}H(d, n)^{3}He, obtained with direct data (blue filled triangles) and with the Trojan Horse method (red filled circles) taken from Tumino et al. (2011). The solid line is an *R*-matrix, fit to both direct and indirect data following the general lines described in Section 2.1. The parameters for an equivalent polynomial fit are listed in Table 2. The vertical dotted line marks the upper value of the energy range of interest for primordial nucleosynthesis.

(A color version of this figure is available in the online journal.)

3.2. $^2H(d, n)^3He$

The *status of the art* before the THM measurement of the ^{2}H(d, n)^{3}He is very similar to its mirror channel. The most relevant data sets are missing in the range between 600 keV and 1 MeV and, in addition, no experimental points in absolute units are present below 6 keV. For this reaction, we have used for our fit to direct data (Greife et al. 1995; Krauss et al. 1987; McNeill & Keyser 1951; Schulte et al. 1972; Jarmie & Brown 1990; Leonard et al. 2006; Ganeev 1957; Arnold et al. 1954; Raiola et al. 2002; Booth et al. 1956; Davidenko 1957; Hofstee et al. 2001; Preston 1954; Belov et al. 1990; Ying et al. 1973; Bystritsky et al. 2010).

The bare nucleus *S*-factor has been obtained from the ^{2}H(^{3}He,n^3He)H by means of the THM (Tumino et al. 2011), and shown in Figure 2, with a 5% experimental error on the whole data set, from 2.6 keV up to 1.5 MeV. The data for the *S*-factor for the reaction, ^{2}H(d, n)^{3}He, obtained with the THM (blue filled triangles) and by different direct measurements (red filled triangles) are shown in Figure 2. The solid line is an *R*-matrix fit to the direct and THM data described in Section 2.1. The parameters for an equivalent polynomial fit, using Equation (7), are listed in Table 2.

3.3. $^3He(d, p)^4He$

The bare-nucleus cross-section for the ^{3}He(d, p)^{4}He fusion reaction, at ultra-low energies, is of interest in pure and applied physics and was measured in the energy region of interest for astrophysics by means of several methods both indirect and direct (Aliotta et al. 2000; Geist et al. 1999; Krauss et al. 1987; Bonner et al. 1952). For the ^{3}He(d, p)^{4}He, we used the direct data from Engstler et al. (1988), Krauss et al. (1987), Bonner et al. (1952), Zhicang et al. (1977), Geist et al. (1999), Moeller et al. (1980), Erramli (2005), Schroeder et al. (1989), and Aliotta et al. (2001). The THM experiment was performed by measuring the ^{3}He(^{6}Li,$p\alpha$)^{4}He reaction in QF kinematics. The bare-nucleus $S(E)$ factor was then extracted in the 0–1 MeV energy range and fitted following Equation (7), as reported in La Cognata et al. (2005). The *S*-factor for the reaction ^{3}He(d, p)^{4}He is shown in Figure 3 with red solid circles for THM data and blue filled triangles for the direct measurements. The solid line is an *R*-matrix fit to the direct and THM data described in Section 2.1. The parameters for an equivalent polynomial plus Breit–Wigner fit are listed in Table 3.

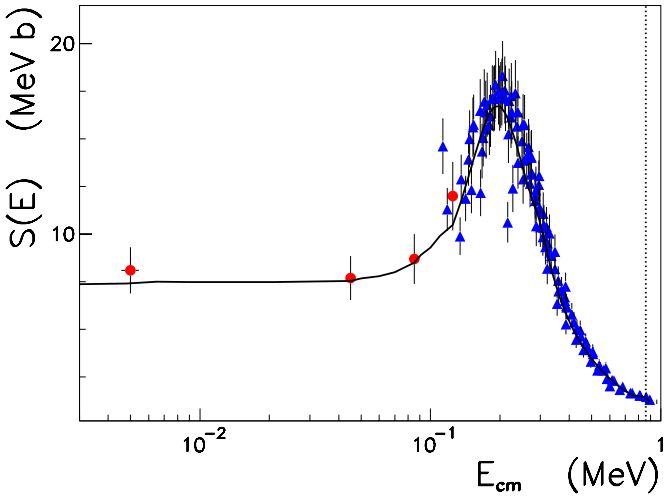

Figure 3. Experimental data for the *S*-factor of the reaction, ^{3}He(d, p)^{4}He, obtained with direct data (blue filled triangles) and with the Trojan Horse method (red filled circles) taken from La Cognata et al. (2005). The solid line is an *R*-matrix fit to both direct and indirect data following the general lines described in Section 2.1. The parameters for an equivalent polynomial plus Breit–Wigner fit are listed in Table 3. The vertical dotted line marks the upper value of the energy range of interest for primordial nucleosynthesis.

(A color version of this figure is available in the online journal.)

3.4. $^7Li(p, \alpha)^4He$

As the main channel of Li burning in astrophysical environments, this reaction is involved in the challenging scenarios of both stellar and primordial Li nucleosynthesis. In such cases,

the discrepancy of about a factor of three between the predictions of SBBN and the Li abundances observed in halo stars represents the well-known and still open "lithium problem." A large number of possible explanations of this discrepancy have been proposed, from stellar phenomena, to non-standard BBN models.

The ^{7}Li$(p, \alpha)^4$He reaction was extensively studied in the last 20 yr both directly (Engstler et al. 1988; Cruz et al. 2009) and indirectly (Lattuada et al. 2001; Pizzone et al. 2003; Lamia et al. 2012b), using the THM. For this reaction, we used the data sets from Schroeder et al. (1989), Mani et al. (1964), Cassagnou et al. (1962), Fiedler & Kunze (1967), Spinka et al. (1971), Rolfs & Kavanagh (1986), Harmon (1989), Engstler et al. (1992), Ciric (1976), Spraker et al. (2000), Lee (1969), and Cruz et al. (2009). The most recent data set for the S-factor for this reaction, obtained with the THM after d QF breakup, are shown in Figure 4 (Lamia et al. 2012a) as red filled circles while the direct ones are reported as blue filled triangles. The solid line is an R-matrix fit to both direct and indirect data following the general lines described in Section 2.1. The parameters for an equivalent polynomial fit are listed in Table 3. The R-matrix fit is then used to calculate the reaction rate following Equation (3), as for the other examined cases.

3.5. Reaction Rates with THM Data

The reaction rates for the four reactions mentioned above (from a compilation of direct and THM data, as reported in the sections above) have been carried out numerically, introducing the R-matrix results in Equation (3). Thus, we fitted the rates with the parameterization displayed in Equation (11). This is the common procedure adopted in previous works (see, e.g., Smith et al. 1993; Cyburt 2004; Coc et al. 2012). For the four reactions of interest, we have included the experimental errors from measurements, allowing us to evaluate the respective errors in the reaction rates. The numerical results are then fitted with the expression

$$N_A \langle \sigma v \rangle = \exp\left[a_1 + a_2 \ln T_9 + \frac{a_3}{T_9} + a_4 T_9^{-1/3} + a_5 T_9^{1/3} + a_6 T_9^{2/3} + a_7 T_9 + a_8 T_9^{4/3} + a_9 T_9^{5/3}\right], \quad (11)$$

which incorporates the relevant temperature dependence of the reaction rates during the BBN. The a_i coefficients for the ^{2}H$(d, p)^3$H and the ^{2}H$(d, n)^3$He reactions are given for both THM and direct measurements as well as for the direct ones (see Section 4 for details) in Table 4, while the coefficients for the ^{3}He$(d, p)^4$He and ^{7}Li$(p, \alpha)^4$He reaction rate expression are given in Table 5. The direct data were considered for energies above 100 keV for ^{3}He$(d, p)^4$He and ^{7}Li$(p, \alpha)^4$He and for energies above 10 keV for ^{2}H$(d, p)^3$H and ^{2}H$(d, n)^3$He, in order to avoid the enhancement due to the electron screening in the direct data.

The ratio between the reaction rates obtained with the THM with those from other compilations are shown in Figures 5 and 6. In these figures, the comparison is made with reaction rates calculated from our own fit to existing direct reaction capture data from the NACRE compilation (Angulo et al. 1999), the Smith et al. (1993) compilation, and the compilation by Cyburt (2004). The error band is associated with the error bars of the associated THM+direct S-factors (Figures 1–4).

For all the cases, we noticed that deviations of up to 20% are obtained from previous compilations. The reaction rate for the ^{3}He$(d, p)^4$He process was not published in the NACRE compilation and, in this case, we use the reaction rate fit as published in Smith et al. (1993). Also, for the reaction ^{7}Li$(p, \alpha)^4$H a large discrepancy with the reaction rate by Cyburt (2004) was found at temperatures above $T_9 \sim 4$.

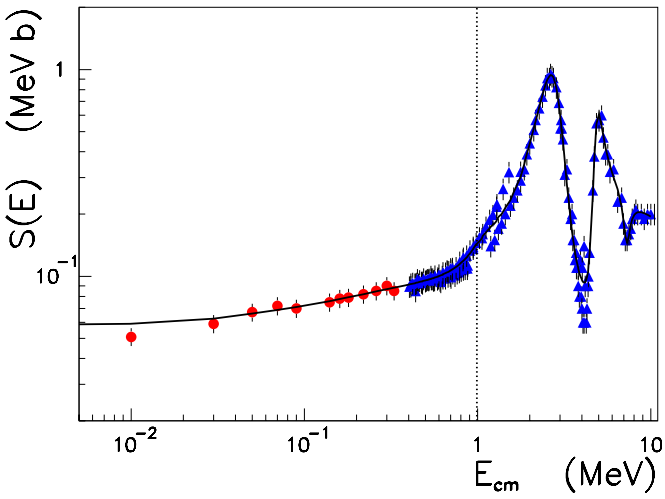

Figure 4. Experimental $S(E)$-factor of the reaction ^{7}Li$(p, \alpha)^4$He obtained with direct data (blue filled triangles) and with the Trojan Horse method (red filled dots) taken from Lamia et al. (2012b). The solid line is an R-matrix fit to both direct and indirect data following the general lines described in Section 2.1. The parameters for an equivalent polynomial fit are listed in Table 3. The vertical dotted line marks the upper value of the energy range of interest for primordial nucleosynthesis.

(A color version of this figure is available in the online journal.)

4. APPLICATION TO BBN

The SBBN is sensitive to certain parameters, including the baryon-to-photon ratio, the number of neutrino families, and the neutron decay lifetime. We use the values $\eta = 6.16 \times 10^{-10}$ for the baryon–photon ratio, the number of neutrino families $N_\nu = 3$, and the neutron lifetime $\tau_n = 878.5$ s, respectively (Steigman 2007, and references therein). Our BBN abundances were calculated with a modified version of the standard BBN code derived fromWagoner et al. (1967), Kawano (1988, 1992).

Although BBN can involve reactions up to the CNO cycle (Coc et al. 2012), the most important reactions, which can significantly affect the predictions of the abundances of the light elements, are listed in Table 1. The reaction rates involving Be, B, C, N, and O isotopes were taken from Wagoner (1969), Caughlan & Fowler (1988), Malaney & Fowler (1989), Wiescher et al. (1989), and Thomas et al. (1993). For the remaining reactions, we have used the compilations by SKM (Smith et al. 1993), NACRE (Angulo et al. 1999), Cyburt (2004), and (Descouvemont et al. 2004 and references mentioned therein). The data for the $n(p, \gamma)d$ reaction was taken from the online ENDF[6] database (see also Cyburt 2004; Ando et al. 2006).

In Figure 7, we show the results for the abundances (mass fraction Y_p for ^{4}He) for ^{2}H, ^{3}He, ^{4}He, ^{6}Li, and ^{7}Li as a function of time. The uncertainties in the experimental nuclear data are reflected in the width of the predicted abundances. In Table 6, the first column is the result obtained with our own fit to the world data from direct measurements. The second column is the impact of replacing the direct data for the reaction ^{2}H$(d, p)^3$H

[6] ENDF/B-VI, online Database at the NNDC Online Data Service, http://www.nndc.bnl.gov

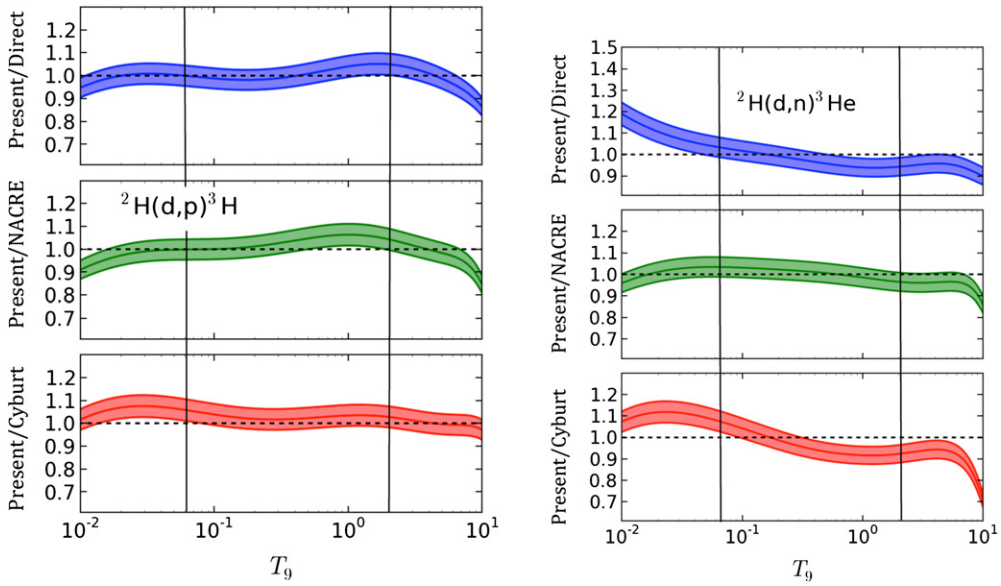

Figure 5. Left: ratio of the ^{2}H(d, p)^{3}H reaction rates calculated using THM data to the one obtained from direct data fits (upper panel). The middle and lower panels are similar ratios using rates published in NACRE (Angulo et al. 1999) and Cyburt (2004). Right: same as in the left figure but for the ^{2}H(d, n)^{3}He reaction. The vertical lines represent the approximated lower and upper temperature limits of interest for big bang nucleosynthesis.

(A color version of this figure is available in the online journal.)

Table 4
Reaction Rate Parameters (Appearing in Equation (11)) for ^{2}H(d, p)^{3}H and ^{2}H(d, n)^{3}He Evaluated from the Present Work and S-factors from Direct Measurements

a_i	^{2}H(d, p)^{3}H (Present)	^{2}H(d, p)^{3}H (Direct)	^{2}H(d, n)^{3}He (Present)	^{2}H(d, n)^{3}He (Direct)
a_1	14.996	20.255	16.1787	13.3209
a_2	−2.4127	−0.63670	−1.9372	−2.9254
a_3	2.8261×10^{-3}	7.7756×10^{-5}	2.0671×10^{-3}	4.0072×10^{-3}
a_4	−5.3256	−4.2722	−5.0226	−5.6687
a_5	6.6125	−1.0758	5.7866	10.1787
a_6	2.4656	2.3211	-2.039×10^{-2}	0.1550
a_7	−3.8702	−1.3062	−0.7935	−2.5764
a_8	1.6700	0.38274	0.2678	1.1967
a_9	−0.25851	-5.0848×10^{-2}	-3.1586×10^{-2}	−0.1807

Table 5
Reaction Rate Parameters (Appearing in Equation (11)) for ^{3}He(d, p)^{4}He and ^{7}Li(p, α)^{4}He Evaluated from Present Work and S-factors from Direct Measurements

a_i	^{3}He(d, p)^{4}He (Present)	^{3}He(d, p)^{4}He (Direct)	^{7}Li(p, α)^{4}He (Present)	^{7}Li(p, α)^{4}He (Direct)
a_1	20.4005	38.9078	17.6686	17.5315
a_2	1.3850	5.9512	−1.1549	−1.397
a_3	-1.2982×10^{-2}	-1.6061×10^{-2}	-4.4059×10^{-4}	6.9425×10^{-4}
a_4	−4.1193	−2.1962	−8.5485	−8.7921
a_5	12.2954	−20.5983	4.6683	5.7430
a_6	−15.2114	1.5636	−0.7858	−2.4092
a_7	5.4147	0.7040	−2.3208	0.6434
a_8	−0.5048	−0.1877	2.0628	1.290
a_9	-4.3372×10^{-2}	2.9419×10^{-2}	−0.4747	−0.3467

by those obtained with the reaction rate calculated in the present work. The subsequent columns are the same, but for the three other remaining measurements. The column labeled "all" uses all four reaction rates calculated in this paper. Finally, the last column lists the observed abundances. The uncertainties in the experimental data are reflected in the errors for the predicted abundances. As expected, the abundance of ^{4}He is barely affected by the new measurements. Also, some of the abundances are not affected by changes in reactions not directly related to the production or destruction of the element. Some appreciable changes in the abundances of d, ^{3}He and ^{7}Li are visible.

The mass fraction for ^{4}He, $Y_p = 0.2565 \pm 0.006$ (0.001 statistical and 0.005 systematic), was obtained from the observation

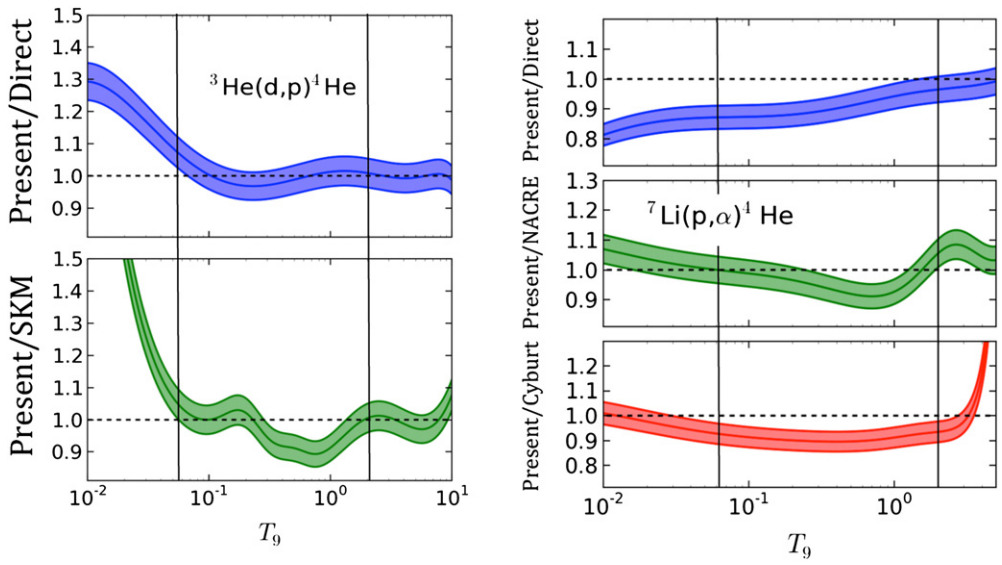

Figure 6. Left: ratio of the ^{3}He(d, p)^{4}He reaction rates calculated using THM data to the one obtained from direct data fits (upper panel). The middle and lower panels are similar ratios using rates published in (Smith et al. 1993; lower panel). Right: in the left figure, ratio of rates calculated using THM (as discussed in the text) to the one obtained with a fit to the direct data (without TH) of the S-factors (upper panel). The middle and lower panels are similar ratios with rates published in NACRE (Angulo et al. 1999) and Cyburt (2004). The vertical lines represent the approximated lower and upper temperature limits of interest for big bang nucleosynthesis.

(A color version of this figure is available in the online journal.)

Table 6
BBN Predictions Using Different Sets of Data (See the Text) Compared with Observations

Yields	Direct	^{2}H(d, p)^{3}H	d(d, n)^{3}He	^{3}He(d, p)α	^{7}Li(p, α)^{4}He	All	Observed
Y_p	0.2486	$0.2485^{+0.001}_{-0.001}$	$0.2485^{+0.000}_{-0.000}$	$0.2486^{+0.000}_{-0.000}$	$0.2486^{+0.000}_{-0.000}$	$0.2485^{+0.001}_{-0.002}$	0.256 ± 0.006[a]
D/H	2.645	$2.621^{+0.079}_{-0.046}$	$2.718^{+0.077}_{-0.036}$	$2.645^{+0.002}_{-0.007}$	$2.645^{+0.000}_{-0.000}$	$2.692^{+0.177}_{-0.070}$	2.82 ± 0.26[b]
^{3}He/H	9.748	$9.778^{+0.216}_{-0.076}$	$9.722^{+0.052}_{-0.092}$	$9.599^{+0.050}_{-0.003}$	$9.748^{+0.000}_{-0.000}$	$9.441^{+0.511}_{-0.466}$	$\geqslant 11. \pm 2.$[c]
^{7}Li/H	4.460	$4.460^{+0.001}_{-0.001}$	$4.470^{+0.010}_{-0.006}$	$4.441^{+0.190}_{-0.088}$	$4.701^{+0.119}_{-0.082}$	$4.683^{+0.335}_{-0.292}$	1.58 ± 0.31[d]

Notes. (a) The mass fraction for ^{4}He, $Y_p = 0.2565 \pm 0.006$ (0.001 statistical and 0.005 systematic), is from Izotov & Thuan (2010). (b) The mean deuterium abundance is the mean average $\langle$(D/H)$\rangle = (2.82 \pm 0.26) \times 10^{-5}$, which is equivalent to $\Omega_b h^2$ (BBN) $= 0.0213 \pm 0.0013$ (O'Meara et al. 2006). (c) The ^{3}He abundances are adopted from Bania et al. (2002) as a lower limit to the primordial abundance. (d) The lithium abundance arises from observations of stars which provide a sample of the "lithium plateau" (Sbordone et al. 2010). D/H is in units of 10^{-5}, ^{3}He/H in 10^{-6} and Li/H in 10^{-10}.

of low-metallicity extragalactic H II regions (Izotov & Thuan 2010). The mean deuterium abundance is $\langle$(D/H)$\rangle = (2.82 \pm 0.26) \times 10^{-5}$, which is equivalent to $\Omega_b h^2$ (BBN) $= 0.0213 \pm 0.0013$ (O'Meara et al. 2006). This average agrees within error bars with $\Omega_b h^2$ (CMB) $= 0.02273 \pm 0.00062$ obtained from the analysis of *WMAP*5 (Dunkley et al. 2009, see also Steigman 2010; Pettini et al. 2008). The ^{3}He abundance is adopted from Bania et al. (2002) as a lower limit to the primordial abundance. The lithium abundance arises from observations of stars which provide a sample of the "lithium plateau" (Sbordone et al. 2010). In Figure 7, the calculated abundance for ^{3,4}He, ^{2}H, and ^{7}Li is reported as a function of time and temperature for the BBN. The band represents the uncertainty derived from the measurements discussed above for each element. The present work gives an exhaustive and updated review of the rate reaction evaluation for some of the relevant reactions for nuclear astrophysics (arising both from direct and indirect methods). We can point out that the discrepancy calculated-to-observed for ^{3}He and ^{7}Li (see Table 6) is still evident, as seen in many other investigations (Steigman 2007) and it seems to not be due to nuclear reaction rate uncertainties.

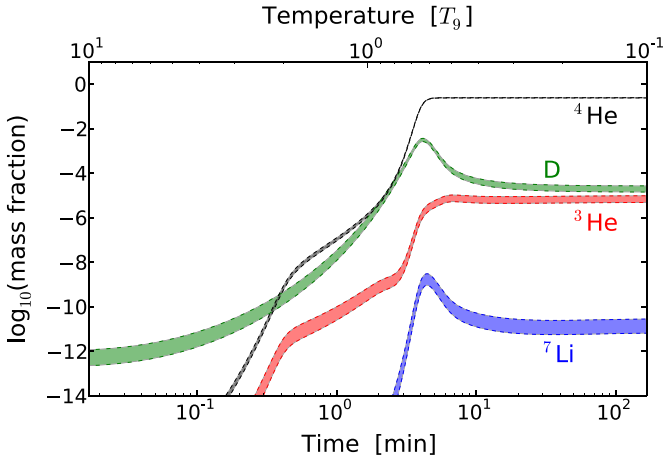

Figure 7. Calculated BBN abundance of ^{3,4}He, D, and ^{7}Li as a function of time and temperature. The black line represents ^{4}He mass fraction, green represents the deuterium abundance, red represents the ^{3}He abundance, and blue represents the ^{7}Li abundance. The error band represents the uncertainty in the THM measurements and their influence on the abundances.

(A color version of this figure is available in the online journal.)

5. DISCUSSION AND CONCLUSION

The reaction rates of four of the main reactions of the BBN network in the temperature range ($0.001 < T_9 < 10$), namely, ^{2}H$(d, p)^3$H, $d(d, n)^3$He, ^{3}He$(d, p)^4$, and ^{7}Li$(p, \alpha)^4$He, have been numerically calculated, including the recent THM measurements. The uncertainties of experimental data for direct and THM data have been fully included for the above reactions. The extension of the same methodology to the other reactions forming the BBN reaction network will be examined in a forthcoming paper. The parameters of each of the reaction rates, as given in Equation (11), are reported in Tables 4 and 5. The obtained reaction rates are compared with some of the most commonly used compilations found in the literature. An updated compilation of direct data for the ^{2}H$(d, p)^3$H, $d(d, n)^3$He, ^{3}He$(d, p)\alpha$, and ^{7}Li$(p, \alpha)^4$He reactions has also been made, and relative expressions for the reaction rate are also given. The reaction rates calculated in the present work are used to calculate the BBN abundance for ^{3,4}He, D and ^{7}Li. The obtained abundances are in agreement, within the experimental errors, with those obtained using the compilation of direct reaction rates. Moreover, a comparison of our predictions with the observations for primordial abundance of ^{3,4}He, D, and ^{7}Li show an agreement for ^{3,4}He and D, while showing a relevant discrepancy for ^{7}Li. The present results show the power of THM as a tool for exploring charged particle-induced reactions at the energies typical of BBN. From Table 6, we can see that the primordial abundances, calculated using the present reaction rates, agree within the uncertainties with the predictions arising from direct data. The comparison between predicted values and observations clearly confirms the discrepancy for ^{7}Li abundance, which is still under debate.

This work was supported by the Italian Ministry of the University under grant No. RBFR082838 and by the Italian Ministry of University MIUR under the grant "LNS Astrofisica Nucleare (fondi premiali)." This work was partially supported by the US-DOE grants DE-FG02-08ER41533 and DE-FG02-10ER41706. A.M. acknowledges the support by US Department of Energy under grant Nos. DE-FG02-93ER40773, DE-FG52-09NA29467, and DE-SC0004958.

REFERENCES

Aliotta, M., Raiola, F., Gyrky, G., et al. 2001, NuPhA, 690, 790
Aliotta, M., Spitaleri, C., Lattuada, M., et al. 2000, EPJA, A9, 435
Ando, S., Cyburt, R. H., Hong, S. W., & Hyun, C. H. 2006, PhRvC, 74, 025809
Angulo, C., Arnould, M., Rayet, M., et al. 1999, NuPhA, 656, 3
Arnold, W. B., et al. 1954, PhRv, 483, 93
Assenbaum, H. J., Langanke, K., & Rolfs, C. 1987, ZPhyA, 327, 461
Azuma, R. E., Uberseder, E., Simpson, E. C., et al. 2010, PhRvC, 81, 045805
Bania, T. M., Rood, R. T., & Balser, D. S. 2002, Natur, 415, 54
Baur, G., Bertulani, C. A., & Rebel, H. 1986, NuPhA, 458, 188
Belov, A. S., Kusik, V. E., & Ryabov, Y. V. 1990, NCimA, 1647, 103
Bertulani, C. A. 2013, Nuclei in the Cosmos (Singapore: World Scientific)
Bertulani, C. A., & Gade, A. 2010, PhR, 485, 195
Bonetti, R., Broggini, C., Campajola, L., et al. 1999, PhRvL, 82, 5205
Bonner, T. W., Conner, J. P., & Lillie, A. B. 1952, PhRv, 88, 473
Booth, D. L., Preston, G., & Shaw, P. F. 1956, PPSA, 265, 69
Bystritsky, V. M., Gerasimov, V. V., Krylov, A. R., et al. 2010, ROIE, 563, 74
Casella, C., Costantini, H., Lemut, A., et al. 2002, NuPhA, 706, 203
Cassagnou, Y., Jeronymo, J., Mani, G. S., Sadeghi, A., & Forsyth, P. D. 1962, NucPh, 449, 33
Caughlan, G. R., & Fowler, W. A. 1988, ADNDT, 40, 283
Ciric, D. M. 1976, Rev. Sci. Res., 115, 6
Coc, A., Goriely, S., Xu, Y., Saimpert, M., & Vangioni, E. 2012, ApJ, 744, 158
Cook, C. F., et al. 1953, PhRv, 785, 89
Cruz, J., Fonseca, M., Luis, H., et al. 2009, NIMPB, 267, 478
Cyburt, R. H. 2004, PhRvD, 70, 023505
Davenport, P. A. 1953, Proc. Royal Society (London) A, 66, 213
Davidenko, V. A. 1957, JNuE, 258, 2
Descouvemont, P., Adahchour, A., Angulo, C., Coc, A., & Vangioni-Flam, E. 2004, ADNDT, 88, 203
Descouvemont, P., & Baye, D. 2010, RPPh, 73, 036301
Dunkley, J., Spergel, D. N., Komatsu, E., et al. 2009, ApJS, 180, 306
Engstler, S., Krauss, A., Neldner, K., et al. 1988, PhLB, 202, 179
Engstler, S., Raimann, G., Angulo, C., et al. 1992, PhLB, 20, 279
Erramli, H. 2005, Phys. and Chem. News (Morocco), 67, 23
Ezer, D., & Cameron, A. G. W. 1963, Icar, 1, 422
Fiedler, O., & Kunze, P. 1967, NuPhA, 513, 96
Fields, B. D., & Sarkar, S. 2006, JPhG, 33, 220
Fowler, W. A., Caughlan, G. R., & Zimmerman, B. A. 1967, ARA&A, 5, 525
Ganeev, A. S. 1957, Suppl. Sov. Atom. J., 5, 26
Geist, W. H., Brune, C. R., Karwowski, H. J., et al. 1999, PhRvC, 60, 054003
Greife, U., Gossis, F., Junker, M., et al. 1995, ZPhy, 351, 107
Gulino, M., Spitaleri, C., Cherubini, S., et al. 2010, JPhys, 37, 125105
Harmon, J. F. 1989, NIMPB, 507, 40
Hofstee, M. A., Pallone, A. K., Cecil, F., et al. 2001, NuPhA, 688, 527
Iliadis, C. 2007, Nuclear Physics of Stars (Wenheim, Germany: Wiley)
Israelian, G. 2012, Natur, 489, 37
Izotov, Y. I., & Thuan, T. X. 2010, ApJL, 710, L67
Jarmie, N., & Brown, R. E. 1990, PhRvC, 41, 1391
Kawano, L. 1988, FERMILAB Report No. PUB-88/34-A (unpublished)
Kawano, L. 1992, STIN, 92, 25163
Kolb, E. W., & Turner, M. S. 1990, The Early Universe (Reading, MA: Addison-Wesley)
Komatsu, E., Smith, K. M., Dunkley, J., et al. 2011, ApJS, 192, 18
Krauss, A., Becker, H. W., Trautvetter, H. P., Rolfs, C., & Brand, K. 1987, NuPhA, 465, 150
La Cognata, M., Mukhamezhanov, A., Spitaleri, C., et al. 2011, ApJL, 739, L54
La Cognata, M., Spitaleri, C., Tumino, A., et al. 2005, PhRvC, 72, 065802
Lamia, L., La Cognata, M., Spitaleri, C., Irgaziev, B., & Pizzone, R. G. 2012a, PhRvC, 85, 025805
Lamia, L., Romano, S., Carlin, N., et al. 2007, NuPhA, 787, 309c
Lamia, L., Spitaleri, C., Burjan, V., et al. 2012b, JPhG, 39, 015106
Lamia, L., Spitaleri, C., La Cognata, M., et al. 2012c, A&A, 541, 158
Lamia, L., Spitaleri, C., Pizzone, R. G., et al. 2013, ApJ, 768, 65
Lattuada, M., Pizzone, R. G., Typel, S., et al. 2001, ApJ, 562, 1076
Lee, C. C. 1969, JKPS, 1, 2
Leonard, D. S., Karwowski, H. J., Brune, C., et al. 2006, PhRvC, 73, 045801
Malaney, R. A., & Fowler, W. A. 1989, ApJL, 345, L5
Mani, G. S., Freeman, R., Picard, F., et al. 1964, NucPh, 588, 60
McNeill, K. G., & Keyser, G. M. 1951, PhRv, 602, 81
Moeller, W., Scherzer, B. M., & Behrisch, R. 1980, NIMPR, 111, 168
Moffat, J. 1952, PPSA, 220, 212
Mukhamezhanov, A., Bem, P., Burjan, V., et al. 2008, PhRvC, 78, 0158042008
Musumarra, A., Pizzone, R. G., Blagus, s., et al. 2001, PhRvC, 64, 068801
O'Meara, J. M., Burles, S., Prochaska, J. X., & Prochter, G. E. 2006, ApJL, 649, L61
Pettini, M., Zych, B. J., Murphy, M. T., Lewis, A., & Steidel, C. C. 2008, MNRAS, 391, 1499
Pizzone, R. G., Spitaleri, C., Bertulani, C. A., et al. 2013, PhRvC, 87, 025805
Pizzone, R. G., Spitaleri, C., Cherubini, S., et al. 2005a, PhRvC, 71, 058801
Pizzone, R. G., Spitaleri, C., Lamia, L., et al. 2011, PhRvC, 83, 045801
Pizzone, R. G., Spitaleri, C., Lattuada, M., et al. 2003, A&A, 398, 423
Pizzone, R. G., Spitaleri, C., Mukhamedzhanov, A., et al. 2009, PhRvC, 80, 025807
Pizzone, R. G., Tumino, A., Deglà Innoccenti, S., et al. 2005b, A&A, 438, 779
Preston, G. 1954, PPSA, 206, 226
Raiola, F., Migliardi, P., Gyurky, G., et al. 2002, EPJA, 13, 377
Rolfs, C., & Kavanagh, R. W. 1986, NuPhA, 179, 455
Romano, S., Lamia, L., Spitaleri, C., et al. 2006, EPJA, 27, 221
Sbordone, L., Bonifacio, P., Caffau, E., et al. 2010, AN, 522, 26
Schroeder, U., Engslter, S., Krauss, A., et al. 1989, NIMPB, 466, 40
Schulte, R. L., Cosack, M., Obst, A., et al. 1972, NuPhA, 192
Sergi, M. L., Spitaleri, C., La Cognata, M., et al. 2010, PhRvC, 82, 032801
Smith, M. S., Kawano, L. H., & Malaney, R. A. 1993, ApJ, 85, 219
Spinka, H., Tombrello, T., & Winkler, H. 1971, NuPhA, 1, 164
Spitaleri, C., Aliotta, M., Cherubini, S., et al. 1999, PhRvC, 60, 055802
Spitaleri, C., Cherubini, S., Del Zoppo, A., et al. 2003, NuPhA, 719, 99c
Spitaleri, C., Mukhamedzhanov, A., Blokhintsev, L., et al. 2011, PAN, 74, 1725
Spitaleri, C., Typel, S., Pizzone, R. G., et al. 2001, PhRvC, 63, 055801
Spraker, M., Prior, R. M., Godwin, M. A., et al. 2000, PhRvC, 015802, 61
Steigman, G. 2007, ARNPS, 57, 463

Steigman, G. 2010, in 11th Symposium on Nuclei in the Cosmos, NIC XI July 19–23, Heidelberg, Germany, http://pos.sissa.it/cgi-bin/reader/conf.cgi?confid=100, id. 1
Thomas, D., Schramm, D. N., Olive, K. A., & Fields, B. D. 1993, ApJ, 406, 569
Tie-Shan, W. 2007, ChPhL, 3103, 24
Tumino, A., Sparta, R., Spitaleri, C., et al. 2014, ApJ, 785, 96
Tumino, A., Spitaleri, C., Bonomo, C., et al. 2005, EPJA, 25, 649
Tumino, A., Spitaleri, C., Mukhamezhanov, A., et al. 2008, PhRvC, 78, 064001
Tumino, A., Spitaleri, C., Mukhamezhanovet, A., et al. 2011, PhLB, 700, 111
Tumino, A., Spitaleri, C., Sergi, M. L., et al. 2006, EPJA, 27, 243
Von Engel, A. 1961, PPSA, 445, 264
Wagoner, R., Fowler, W. A., & Hoyle, F. 1967, ApJ, 148, 3
Wagoner, R. V. 1969, ApJS, 162, 247
Wen, Q., Chengbo, L., Zhuo, S., et al. 2008, PhRvC, 78, 035805
Weymann, R., & Moore, E. 1963, ApJ, 137, 552
Wiescher, M., Steininger, R., & Kappeler, F. 1989, ApJ, 344, 464
Ying, N., Cox, B., Barnes, B. K., et al. 1973, NuPhA, 481, 206
Zhicang, L., et al. 1977, At. Energy Sci. Tecnol., 229, 11